Multiple subduction imprints in the mantle below Italy detected in a single lava flow

Citation for published version:
Nikogosian, IK, Ersoy, O, Whitehouse, M, Mason, PRD, De Hoog, C-J, Wortel, R & Van Bergen, MJ 2016, 'Multiple subduction imprints in the mantle below Italy detected in a single lava flow' Earth and Planetary Science Letters, vol 449, pp. 12-19. DOI: 10.1016/j.epsl.2016.05.033

Digital Object Identifier (DOI):
10.1016/j.epsl.2016.05.033

Published In:
Earth and Planetary Science Letters

Multiple subduction imprints in the mantle below Italy detected in a single lava flow

Igor Nikogosian*[a], Özlem Ersoy[a], Martin Whitehouse[b], Paul R.D. Mason[a], Jan C.M. de Hoog[c], Rinus Wortel[a] and Manfred J. van Bergen[a]

* corresponding author: i.nikogosian@vu.nl

[a] Department of Earth Sciences, Utrecht University, Budapestlaan 4, 3584 CD Utrecht, The Netherlands

[b] Swedish Museum of Natural History, Box 50007, SE104 05 Stockholm, Sweden

[c] School of GeoScience, University of Edinburgh, West Mains Road, EH9 3JW, Edinburgh, United Kingdom

Abstract

Post-collisional magmatism reflects the regional subduction history prior to collision but the link between the two is complex and often poorly understood. The collision of continents along a convergent plate boundary commonly marks the onset of a variety of transitional geodynamic processes. Typical responses include delamination of subducting lithosphere, crustal thickening in the overriding plate, slab detachment and asthenospheric upwelling, or the complete termination of convergence. A prominent example is the Western-Central Mediterranean, where the ongoing slow convergence of Africa and Europe (Eurasia) has been accommodated by a variety of spreading and subduction systems that dispersed remnants of subducted lithosphere into the mantle, creating a compositionally wide spectrum of magmatism. Using lead isotope compositions of a set of melt inclusions in magmatic olivine crystals we detect exceptional heterogeneity in the mantle domain below Central Italy, which we attribute to the presence of continental material, introduced initially by Alpine and subsequently by Apennine subduction. We show that superimposed subduction imprints of a mantle source can be tapped during a melting episode millions of years later, and are recorded in a single lava flow.

Keywords: Melt inclusions, Pb isotopes, mantle heterogeneity, Italian magmatism, Mediterranean geodynamics, Latera volcano

1. Introduction

Despite its relative rarity, post-collisional potassium-rich magmatism provides important insight into the composition of the subcontinental lithospheric mantle along the Alpine-Himalayan belt, and highlights the role of recycled continental-crust (Guo et al., 2006; Lustrino et al., 2011; Miller et al., 1999; Prelević et al., 2013; Tommasini et al., 2011; Zhao et al., 2009). Extensive studies of Italian mainland volcanics have used Sr-Nd-Pb isotopes to argue for involvement of recycled crustal material (Conticelli et al., 2002; Lustrino et al., 2011; Peccerillo, 1999), but in view of the complex subduction history of the Mediterranean region, the provenances are difficult to resolve using bulk-rock samples. Melt inclusions (MIs) provide direct information about primitive magma compositions in considerably more detail (Jackson and Hart, 2006; Kobayashi et al., 2004; Maclennan, 2008; Nikogosian and van Bergen, 2010; Rose-Koga et al., 2012; Saal et al., 2005; Sobolev et al., 2000; Sorbadere et al., 2012). We use olivine-hosted MIs from Latera, a strategically positioned volcano in Central Italy, to investigate the subcontinental mantle source beneath the Italian peninsula. We demonstrate that their Pb isotope compositions and trace-element signatures are diagnostic in tracing input from both Alpine and Apennine subduction.

1.1. Magmatic and geodynamic setting

Pliocene to present-day magmatism in peninsular Italy has developed in a post-collision setting associated with plate convergence involving continental Europe, the extending western Mediterranean realm and Adriatic-Ionian lithosphere (Fig. 1).

The large compositional spectrum of predominantly potassic parental magmas has been attributed to (1) different subducted crustal components, (2) heterogeneous premetasomatic mantle or (3) progressive melt-extraction processes (Conticelli et al., 2004; Foley, 1992; Peccerillo, 2005).

Further to this, systematic compositional variation in erupted products with geographic location could reflect lateral heterogeneity in mantle sources affected by distinct metasomatic events associated with multiple subduction systems (Peccerillo, 1999). Magmatism in and off the northern part of peninsular Italy (mostly in the Tuscany-Corsica region) has been linked to Cretaceous-Oligocene Alpine subduction (Peccerillo, 1999; Peccerillo and Martinotti, 2006) and is characterized by lamproite (LAM) - shoshonite (SHO) - calc-alkaline (CA) magmatic associations. In contrast, magma sources in Central-Southern Italy developed under the influence of the Miocene to Recent subduction of Adriatic-Ionian lithosphere and produced shoshonite and strongly silica-undersaturated leucite-bearing high-potassium (HKS) and minor subalkaline rock series (Conticelli et al., 2002; Peccerillo, 1999).

Seismic tomography has identified the presence of fossil and still actively subducting slabs below Italy, related to the south- to eastward subduction of Tethyan oceanic lithosphere in the north, and the southwest to westward subduction of Adriatic and Ionian lithosphere, with continental and oceanic affinities respectively, below the central and southern areas (Giacomuzzi et al., 2012; Spakman and Wortel, 2004). These two separate subduction processes are referred to as Alpine and Apennine subduction, respectively (see Fig. 1). The geodynamic influence on magmatism is further complicated by rollback, tearing, and detachment of slabs and lithospheric delamination that accompanied subduction of the Adriatic lithosphere in the Apennine subduction zone (Chiarabba and Chiodini, 2013; Faccenna et al., 2001; Giacomuzzi et al., 2012; Serri et al., 1993; Wortel and Spakman, 2000).

Latera stratovolcano represents the latest stage (0.28-0.15 Ma) of K-rich volcanism in the Vulsini volcanic complex (< 0.7 Ma), the northernmost sector of the Roman Magmatic Province (Roman MP) where HKS and SHO rock series prevail (Peccerillo, 2005). In this area, the Roman MP overlaps the neighboring Tuscan Magmatic Province (Tuscan MP) (Fig. 1) where mantle-derived magmas are represented by LAM-SHO-CA associations (Conticelli et al., 2010). Erupted products of Latera comprise SHO as well as HKS rock types (Conticelli et al., 1991). We focus on samples from various locations across a ca. 12 km long shoshonitic flow (Selva del Lamone, SdL) and from a representative HKS lava from nearby Monte Starnina (Conticelli et al., 1991). The SdL samples (4.8-5.8 wt.% MgO) contain olivine phenocrysts together with clinopyroxene, plagioclase, and rare sanidine. The Monte Starnina sample (4.8 wt.% MgO) contains clinopyroxene leucite and olivine as phenocrysts (see Table B.1, Fig. A.1).

2. Methods

2.1. Analytical techniques

Whole-rock compositions of the studied samples were determined by XRF (major elements) and ICP-MS (trace elements) at the Earth Science Department of the Free University (Amsterdam), using a Philips PW1404/10 and Thermo Electron X-series II ICP-MS, respectively. Each sample was crushed and sieved to separate the olivine phenocrysts. They were embedded in epoxy holders and polished on one side for electron microprobe analysis (EPMA). The most forsterite-rich olivine grains with noticeable melt inclusions were selected to determine compositions and crystallization conditions of the parental melts. Melt inclusion re-homogenization and quenching experiments were performed with a high-T heating/quenching stage (design of Sobolev et al., 1980) at the Free University (Amsterdam), following the experimental procedure described in Nikogosian and van Bergen (2010). Details of melt inclusions homogenization experiments can be found in Appendix A. After quenching, host-olivine grains were polished until the melt inclusions were exposed at the surface for major, trace, and volatile element analysis by EPMA, Secondary Ion Mass Spectrometry (SIMS), and Laser Ablation Inductively Coupled Plasma Mass Spectrometry (LA-ICP-MS).

EPMA analyses were carried out using a JEOL JXA8600 Superprobe at Utrecht University, operated in WDS (wavelength dispersive) mode following the procedure described in De Hoog et al. (2001). Natural minerals, metals, and synthetic oxides were used as calibration standards. Daughter mineral phases in un-homogenized melt inclusions exposed at the surface were identified using semi-qualitative energy dispersive spectrometry (EDS) analysis.

Low-temperature microthermometry on fluid phases was performed on a Linkam TP/91-THMS 600 stage at the Free University (Amsterdam) following a routine as outlined in Nikogosian et al. (2002).

Concentrations of trace elements in most of the quenched melt inclusions were determined by SIMS using a CAMECA IMS4f at the Institute of Microelectronics (Yaroslavl', Russia), following techniques and procedures reported by Danyushevsky and Sobolev (1996) and Portnyagin et al. (2007). Polished, gold-coated olivine mounts were initially sputtered with a 70 µm diameter primary $^{16}O_2^-$ beam for 3 minutes to remove the coating. Data were obtained using a $^{16}O_2^-$ primary ion beam of 15-20 nA accelerated to 50 kV resulting in a spot size of ca. 10-20 µm. Each MI was analyzed near its center, with 5 data points taken over a 10–15 µm deep vertical profile with an integration time of 40 to 60 minutes. A calibration curve for glass standards ATHO-Ga (Jochum et al., 2006) and NIST SRM 610(Jochum et al., 2011) was used to calculate element concentrations based on the ratio of the respective isotopes to ^{30}Si. Glass standards were analyzed after each 3-6 MI analyses. Data reproducibility is given in Table B.5.

Some of the additional quenched melt inclusions were analyzed for trace element contents by LA-ICP-MS using a GeoLas 200Q Excimer laser ablation system (193 nm wavelength) coupled to a Thermo Finnigan Element 2 sector field ICP-MS instrument at Utrecht University following the techniques of Mason et al. (2008). Data were obtained using a constant fluence of 5-10 J cm^{-2} and pulse repetition rate of 10 Hz with 20-60 µm diameter craters. Each MI was ablated for ca. 25-30s, and background count rates were measured prior to and after the ablation of MI. Calcium determined by EPMA was used as an internal standard, with NIST 612 as the calibration standard.

Lead isotope compositions of MI were acquired by SIMS with a large geometry Cameca-1270 ion microprobe at the NORDSIM Facility, Swedish Museum of Natural History, Stockholm closely following the methods described by Whitehouse et al. (2005). The samples (polished grain mounts) were gold coated to avoid charging during the sputtering process. Data were obtained using a $^{16}O_2^-$ primary ion beam of 20 nA accelerated to 22.5 kV, resulting in a spot size of ca. 20 µm. Following an initial pre-sputter with a rastered beam to remove the gold coating, the secondary ion beam was automatically centered in the 4000 µm field aperture. An energy window of 45 eV was used without applying an energy offset. The instrument was operated in multi-collection mode with simultaneous determination of all four Pb isotopes in low noise ion-counting electron multipliers set on movable trolleys. $^{204}Pb^+$ was measured in the electron multiplier (EM) set on the trolley position L2, $^{206}Pb^+$ in C, $^{207}Pb^+$ in H1, and $^{208}Pb^+$ in H2. A mass resolution of 4860 (M/ΔM) ensured adequate resolution from molecular interferences in the melt inclusions and reference glasses. Mass calibration was performed at the beginning of each analysis based on the ^{208}Pb signal. Each analysis consisted of 100 cycles with a total integration time of 1000 seconds for each isotope. Using the above setup, instrument sensitivity on ^{208}Pb was ca. 30 cps/ppm/nA.

The USGS glass BCR-2G was used as the primary standard to correct for variations in detector efficiency and instrumental mass fractionation. Glasses GSE1-G, BHVO2-G, and BIR1-G were used as secondary standards to monitor the accuracy of the calibration, based on preferred values listed by Georem (Table B.6). Results for the secondary standards were within error of published values for all ^{204}Pb-based ratios. As expected from counting statistics, a strong correlation between Pb concentrations of MI and analytical uncertainty in Pb isotope ratios was observed. Lead concentrations in melt inclusions were sufficiently high so that ^{204}Pb-based ratios could be used for distinction of geochemical sources. Our in run precision ranged from 0.03 to 0.40 (2σ) for ^{206}Pb/^{204}Pb, from 0.03 to 0.35 (2σ) for ^{207}Pb/^{204}Pb and from 0.07 to 0.85 (2σ) for ^{208}Pb/^{204}Pb. A total of 19 melt inclusions were analyzed for Pb isotope compositions, two of which were discarded based on high analytical uncertainties (>0.5 for ^{206}Pb/^{204}Pb) due to primary beam instability during the analysis of these two particular inclusions. Lead concentrations, isotopic ratios, and precision data are provided in Table A.3 for the complete dataset.

3. Results

The SdL flow contains two different magmatic olivine populations (Group-1 and Group-2) that we distinguish by their morphology, chemistry and compositions of trapped melt and spinel inclusions (Tables B.2-B.4, Figs A.1-A.3), as well as rare mantle olivine xenocrysts. Group-1 olivines are characterized by the highest forsterite (Fo_{85}-Fo_{91}), and by relatively low CaO (0.20-0.33 wt.%) and high NiO (0.15-0.40 wt.%) contents that tend to increase with increasing Fo. These euhedral phenocrysts host partially crystallized primary MIs in the 10-80 µm diameter range. Group-2 olivines have overlapping forsterite (Fo_{80}-Fo_{90}), somewhat higher CaO (0.27-0.35 wt.%), and similar NiO contents relative to Group-1. They host large, fully crystallized primary MIs (>100 µm in diameter) with large fluid bubbles, whereas smaller-sized MIs (10-20 µm) are also present.

The chemistry of the MIs corroborates the distinction between the two groups. Although all contain 7-11 wt.% MgO, have a SHO composition, and an overlapping range in potassium (1.7-4.8 wt.% K_2O), Group-1 MIs have lower SiO_2, Al_2O_3, Na_2O, FeO and higher CaO, TiO_2, P_2O_5 and volatile contents than Group-2 MIs. In addition, the MIs show opposite K_2O-CaO relationships (Fig. 2). In both cases, trace element patterns of MIs (Fig. A.4) are overall similar and typical for subduction-related imprints of the mantle sources below peninsular Italy (e.g., Peccerillo, 2005). Group-2 melts are relatively enriched in Zr, Hf, and Pb and depleted in Sr, features that they share with Tuscan lamproites (Fig. A.4; cf., Conticelli et al., 1991; Conticelli et al., 2010; Peccerillo, 2005). Compositions of SdL Group-1 melt inclusions are typical for the shoshonite series (SiO_2=46.9-50.4, MgO=7.1-9.5, K_2O=1.7-3.5 wt.%). Decreasing K_2O is accompanied by a strong increase in CaO (9.3-14.6 wt.%, Fig. 2) and modest decreases in Na_2O (3-1.8 wt.%) and Al_2O3 (17.6-15.1 wt.%), while there are no systematic relations with MgO, SiO_2, TiO_2 (Fig.A.5) or volatile elements (Cl, S, F). Trace element patterns, normalized to depleted MORB mantle (Fig. A.4), display depletion in HFSE relative to LILE and LREE, and enrichments in LREE relative to HREE. These characteristics are typical for all potassic rocks of Central-Southern Italy and are taken to reflect subduction-related enrichments of their mantle sources (Peccerillo, 2005).

Compositions of SdL Group-2 MIs are also predominantly shoshonitic (SiO_2 =48.3-55.4, MgO=7.7-13, K_2O=2.3-4.7 wt.%) but cover a wider K_2O range and have significantly lower CaO contents (1.9-6.9 wt.%) than those of Group-1. The Group-2 MIs have also higher SiO_2, Al_2O_3, Na_2O, FeO, and lower TiO_2, P_2O_5 and volatile contents (Fig2, Fig.A.5). Unlike Group-1, decreasing in K_2O is associated with decreasing CaO (Fig.2), as well as decreasing Na_2O (3.4-1.8 wt.%) and modest increases in MgO and Al_2O_3 (14-22 wt. %), while there are no obvious relationships with SiO_2, TiO_2, P_2O_5 or volatile elements. Trace elements patterns are marked by strong enrichments in Rb, Th, U, Pb, LREE and HFSE, higher La/Yb and Th/Nb, and lower Sm/Yb ratios in comparison to Group-1 MI (Fig. A.4). They also display a Sr depletion and Zr, Hf enrichments. The Group-2 MIs share these features with Tuscan lamproitic lavas (cf., Conticelli et al., 1991; Peccerillo, 2005; Conticelli et al., 2010), but they differ in terms of their overall lower incompatible trace-element contents and stronger Pb enrichment. Melt inclusions with mixed Group-1 and Group-2 compositions were occasionally observed in the rims of Group-2 olivines but are rare in Group-1 olivines.

The compositions of spinel inclusions also confirm the grouping of their olivine hosts. In Group-1 they have slightly lower Cr-numbers [Cr#=Cr/(Cr+Al)] than in Group-2 (0.36-0.46 and 0.45-0.55, respectively; see Fig. A.3), as well as lower Cr_2O_3, TiO_2 and Fe^{2+}/Fe^{3+}, and higher Mg#, Al_2O_3 and MnO. The major and trace element compositions of the HKS MIs closely resemble those of mafic HKS lavas from East Vulsini (Fig. 2, Fig. A.6) testifying that HKS lavas of Latera and adjacent centers in the northernmost sector of the Roman MP are co-genetic (cf., Conticelli et al., 1991).

Of the 19 MIs analyzed for Pb isotopes, 17 had Pb concentrations allowing isotope ratio measurements, including ^{204}Pb, with minimal error (Fig. A.7). Melt inclusions show extreme Pb isotopic diversity (Fig. 3) compared to the narrow range for the host lavas. Group-1 MIs display a remarkable range in isotope ratios between highly unradiogenic and highly radiogenic values for $^{207}Pb/^{204}Pb$ (14.57-16.04) and $^{208}Pb/^{204}Pb$ (36.16-40.44) at $^{206}Pb/^{204}Pb$ values of 17.91-19.29. The Pb isotope ratios of Group-2 MIs are less variable and distinctive with higher $^{207}Pb/^{204}Pb$ and lower $^{206}Pb/^{204}Pb$ relative to the Group-1 trend. The combination of low $^{206}Pb/^{204}Pb$ (18.28-18.30) and $^{208}Pb/^{204}Pb$ (38.02-38.79), and moderately high $^{207}Pb/^{204}Pb$ (15.56-15.72) in Group-2 MIs has not been observed previously in any of the Italian potassic lavas. Together with the two extremes in the Group-1 trend, Group-2 forms three end-member components that make up the bulk-lava composition in Pb isotope space. The Pb isotope compositions of MIs from the HKS lava also display considerable variation ($^{206}Pb/^{204}Pb$=18.51-19.16; $^{207}Pb/^{204}Pb$=15.46-15.80; $^{208}Pb/^{204}Pb$=38.58-39.54), but cover a narrower span. They tend to fall in the Group-1 trend and are close to those of the Vulsini HKS lavas.

4. Discussion

The populations of Fo-rich olivines and their MIs with a large variation in K_2O are difficult to reconcile with simple crystal fractionation (Fig. A.7) and point to mingling between partly crystallized (near-)primary magmas indicating that the SdL lava is a product of different parental melts (ca. 80% Group-1 and 20% Group-2, estimated from mass balance based on trace element concentrations) (Fig. 2, Fig. A.5), derived from two distinctive and heterogeneous mantle sources. Further association with the Monte Starnina lava, a typical example of Roman HKS magmatism in Vulsini (Conticelli et al., 2004), underscores the exceptional compositional diversity of the subcontinental lithospheric mantle beneath Latera, and typifies its complexity on a regional scale.

4.1. Provenances of Subduction-Related Contaminants of the Mantle Source

Mantle sources of the Roman MP have been affected by input of marl-rich sediments through subduction of the continental sector of the Adriatic-Ionian domain in Tertiary times (e.g., Serri et al., 1993). Tuscan MP sources, by contrast, have been influenced by other upper crustal materials associated with the earlier Alpine collision (Peccerillo, 1999; Peccerillo and Martinotti, 2006), and possibly by northward drifted, Gondwana-derived continental slivers piled up by even older collisional events (Tommasini et al., 2011). Pb isotopes measured in bulk mafic lavas from Tuscan MP as well as the northernmost Roman MP confirm this source contamination by upper continental crust (Conticelli et al., 2010; Peccerillo, 2005), but they show insufficient contrast to discriminate between possible provenances of input materials, particularly in the region of overlap between these provinces. The same limitation applies to the SdL lava having Pb isotope ratios close to those reported for the Roman HKS lavas (Fig. 3c).

Our Pb isotope data in MIs from the SdL lava reveal two distinctive trends (Fig. 3), not visible in the bulk rock data. The Group-1 trend extends towards not previously seen extreme $^{207}Pb/^{204}Pb$ and $^{208}Pb/^{204}Pb$ values. One end points towards a radiogenic end-member that could have been introduced through source contamination with upper continental crust. We explain the unradiogenic end-member of the Group-1 melt inclusions by involvement of ancient lower continental crust as a mantle contaminant. Its comparatively high $^{206}Pb/^{204}Pb$ ratio relative to old lower crust (Kramers and Tolstikhin, 1997) implies that this signature must have been created in multiple stages. A plausible scenario is that this crustal contaminant derived from a source in which the Pb isotopic evolution had been retarded relative to single-stage model mantle reservoirs. Such an exotic composition requires an extensive amount of time for Pb ingrowth implying a time of separation in the early Archean, after which an increased U/Pb ratio through intracrustal differentiation ultimately produced the higher $^{206}Pb/^{204}Pb$ signature. The present-day Pb isotope composition of this Group-I endmember is exotic for modern mantle-derived igneous rocks, but it overlaps with Late Archean granitoids from West Greenland (Fig. 3a) that represent re-melting of a lower crustal mafic source or gneissic precursor (Moorbath et al., 1981; Næraa et al., 2014). We therefore surmise that material with an analogous history was introduced in the source of Latera volcano. This would be consistent with the inference that dismembered blocks of an Archean microcontinent in the central-western Mediterranean realm have been involved in collisions with passive margins and the development of subduction-related volcanic arcs during the Tertiary convergence of Africa and Europe (González-Jiménez et al., 2013). The associated mantle source contamination may have occurred through delamination of subducted continental lithosphere or subduction erosion of the overriding plate (cf., Kay and Kay, 1993; Lustrino et al., 2000; Lustrino, 2005). Contamination of mantle sources by ancient lower continental crust with multistage isotopic evolution has not been previously seen in the post-collisional magmatism of peninsular Italy but has been inferred from volcanics in Sardinia (Lustrino et al., 2007).

In terms of Pb isotopes, MIs of the Monte Starnina HKS lava are virtually indistinguishable from Group-1 MIs. The isotopic variability, whilst less than that in Group 1, remains considerable in comparison to bulk data, and overlaps the field of Roman MP HKS lavas (Fig. 3c). Since there is a broad consensus that Roman MP HKS sources were affected by subducted components from Adriatic lithosphere (Peccerillo, 2005), we infer that upper continental metasomatic imprints in the mantle below Latera were predominantly derived from this input. We suggest that the lower continental crust input seen in the Group-1 MIs was introduced by delamination of Adriatic lithosphere as observed in recent seismic tomographic studies (e.g., Giacomuzzi et al., 2012). A similar case where Pb isotopic signatures of magma sources were determined by different portions of a subducted continental margin has been inferred for the arc-continent collision sector in the Sunda-Banda arc (Elburg et al., 2004).

Group-2 MIs (Fig. 3c) are distinctive and point to the presence of a metasomatic component in the Latera mantle source with a separate origin. Ratios for trace elements of comparable incompatibility confirm the compositional dissimilarity of the post-metasomatic mantle source (Fig. 2d). The Pb-isotope compositions (unradiogenic ^{206}Pb, moderately radiogenic ^{207}Pb and ^{208}Pb) are similar to lower continental crust found in the Variscan and older basement of Sardinia and Calabria. They are also close to the composition of Permian sandstones in the Southern and Eastern Alps, representing erosion products of the Variscan orogeny. These similarities strongly suggest that the Group-2 mantle component has an isotopic affinity to ancient lithologies with a paleogeographic position that allowed their involvement in the early-Tertiary Alpine subduction as: (1) erosion products of exhumed basement on top of Ligurian-Provençal oceanic lithosphere (Malavieille et al., 1998), (2) subducted continental lithosphere (Handy et al., 2010) or (3) via subduction erosion of the overriding continental crust (Peccerillo and Martinotti, 2006). The near-vertical trend in Group-2 (Fig. 3c) might indicate mixing between this component and the unradiogenic end-member of Group-1 in Latera's mantle source.

An "Alpine" origin has also been proposed for the Tuscan MP lamproites where melts were derived from mantle sources with a crustal metasomatic imprint obtained during the southeastwards Alpine subduction of Tethyan lithosphere under northern Italy (Peccerillo and Martinotti, 2006). This hypothesis fits with the inference that western Mediterranean lamproites inherited their isotopic variations largely from the provenance and age of continent-derived magma source components that were recycled into the mantle by the Alpine subduction, with Hercynian Europe acting as a passive margin (Prelević et al., 2008). In keeping with this, the unradiogenic ^{206}Pb signature detected at Latera in Group-2 and its correspondence to the fields for Sardinian/Calabrian basement and Alpine sandstones suggest that the earliest introduced source component was subducted erosion products of Variscan or older lithologies. We therefore infer that, relative to the Group-1 MI trend, minor shifts towards lower $^{206}Pb/^{204}Pb$ values in lavas from the northern Roman MP and the Tuscan MP (Fig. 3c) reflect relict components in sub-Apennine mantle sources that were subducted during the Alpine event, in addition to the prevailing components supplied later by the Apennine subduction. Our findings reveal that bulk-lava data should be regarded as mixtures of isotopically contrasting components, and that Pb isotope signatures of MIs can depict the provenance of metasomatic components in the mantle below Central Italy in greater detail.

4.2. Geodynamic Framework

To further explore the connection between post-collisional magmatism and geodynamics we combine our provenance results with independent geophysical evidence concerning the mantle structure and geodynamic evolution of the region. Figure 1b shows that the Latera site is located just above a tear in the subducted slab as inferred from seismic tomography using P-wave delay times (Spakman and Wortel, 2004). Northwest of the tear, the Northern Apennines slab appears to be continuous, whereas to the southeast, the tomographic images indicate detachment of the subducted slab (cf., Wortel and Spakman, 2000).

Latera's peculiar location with respect to this underlying mantle structure implies that magma source components and melt generation should be considered in a true 3D context. Lateral contributions are to be expected from both sides of the tear, corresponding with the Northern and Central Apennines plate boundary segments, respectively. Moreover, the position close to approximately overlapping Adriatic and fossil Alpine lithosphere slabs (Fig. 1b) corroborates the inferred magma derivation from sources affected by metasomatic contributions from both, either superimposed in the same mantle domain or stratigraphically separated. Our data provide no evidence for an asthenospheric contribution from below the Adriatic slab (cf., Rosenbaum et al., 2008).

The melting trigger at Latera was probably the same as that responsible for magmatism in the entire Roman MP. The more easterly advance of the Northern Apennines front relative to that of the Central-Southern Apennines has been suggested to indicate differential retreat of the corresponding slab segments in Late-Pliocene-Quaternary times (Scrocca, 2006). In this context we propose that a sudden and massive advection of heat, associated with the upwelling of hot asthenospheric material in response (Faccenna et al., 2010; Levin et al., 2002) to the segmentation, breaking off and sinking of the central(-southern) Apennines slab (see Fig. 1b), was the magma generating process in the heterogeneous mantle column that produced Latera's SHO and HKS flows. Cooling of the asthenospheric material after upwelling and exhaustion of the metasomatized domains with relatively low melting temperature accounted for the short-lived nature of the Roman Province magmatism, including that of Latera volcano.

5. Conclusions

Multiple associations of olivine phenocrysts and inclusions of spinel and primitive melt within lavas of Latera volcano demonstrate a strong vertical heterogeneity in the mantle below the region of overlap between the Roman and Tuscan Magmatic Provinces (Central Italy). Co-existence of shoshonitic and lamproite-like assemblages in a single lava flow, and proximity to coeval silica-undersaturated ultrapotassic products point to simultaneous extraction of melts from mantle domains with different subduction-related metasomatic signatures.

Extremely variable Pb-isotope compositions of melt inclusions reveal multiple origins for metasomatic agents that remain unnoticed in data from bulk lava samples. We distinguish end-members that agree with subducted continental components with an Alpine inheritance and with derivation from Adriatic upper as well as ancient lower continental crust. Hence, in line with independent geodynamic evidence, our data from Latera volcano expose superimposed imprints from the fossil Alpine and the Apennines subduction systems in the subcontinental mantle of Central Italy. We propose that melting was caused by a thermal pulse associated with upwelling of hot asthenospheric material, triggered by opening of a slab window after segmentation of the Apennines slab and detachment and sinking of the central Apennines slab segment.

Acknowledgments

Our manuscript benefited from critical and constructive comments of two anonymous reviewers. This project was financially supported by the Netherlands Research Centre for Integrated Solid Earth Sciences (ISES)**.**

References

Caron, C., Lancelot, J., Omenetto, P., Orgeval, J., 1997. Role of the Sardic tectonic phase in the metallogenesis of SW Sardinia (Iglesiente); lead isotope evidence. Eur. J. Mineral. 9, 1005-1016.

Chiarabba, C. and Chiodini, G., 2013. Continental delamination and mantle dynamics drive topography, extension and fluid discharge in the Apennines. Geology. 41, 715-718.

Conticelli, S., D'Antonio, M., Pinarelli, L., Civetta, L., 2002. Source contamination and mantle heterogeneity in the genesis of Italian potassic and ultrapotassic volcanic rocks: Sr–Nd–Pb isotope data from Roman Province and Southern Tuscany. Mineral. Petrol. 74, 189-222.

Conticelli, S., Francalanci, L., Santo, A., 1991. Petrology of final-stage Latera lavas (Vulsini Mts.): mineralogical, geochemical and Sr-isotopic data and their bearing on the genesis of some potassic magmas in central Italy. J. Volcanol. Geotherm. Res. 46, 187-212.

Conticelli, S., Laurenzi, M. A., Giordano, G., Mattei, M., Avanzinelli, R., Melluso, L., Tommasini, S., Boari, E., Cifelli, F., Perini, G., 2010. Leucite-bearing (kamafugitic/leucititic) and-free (lamproitic) ultrapotassic rocks and associated shoshonites from Italy: constraints on petrogenesis and geodynamics. J. Virtual Explor. 36.

Conticelli, S., Melluso, L., Perini, G., Avanzinelli, R., Boari, E., 2004. Petrologic, geochemical and isotopic characteristics of potassic and ultrapotassic magmatism in central-southern Italy: inferences on its genesis and on the nature of mantle sources. Period. Mineral. 73, 135-164.

Danyushevsky, L. and Sobolev, A., 1996. Ferric-ferrous ratio and oxygen fugacity calculations for primitive mantle-derived melts: calibration of an empirical technique. Mineral. Petrol. 57, 229-241.

De Hoog, J. C. M., Mason, P. R. D., van Bergen, M. J., 2001. Sulfur and chalcophile elements in subduction zones: constraints from a laser ablation ICP-MS study of melt inclusions from Galunggung Volcano, Indonesia. Geochim. Cosmochim. Acta. 65, 3147-3164.

Elburg, M. A., Van Bergen, M., Foden, J. D., 2004. Subducted upper and lower continental crust contributes to magmatism in the collision sector of the Sunda-Banda arc, Indonesia. Geology. 32, 41-44.

Faccenna, C., Becker, T. W., Lallemand, S., Lagabrielle, Y., Funiciello, F., Piromallo, C., 2010. Subduction-triggered magmatic pulses: A new class of plumes? Earth Planet. Sci. Lett. 299, 54-68.

Faccenna, C., Becker, T. W., Lucente, F. P., Jolivet, L., Rossetti, F., 2001. History of subduction and back arc extension in the Central Mediterranean. Geophys. J. Int. 145, 809-820.

Foley, S., 1992. Vein-plus-wall-rock melting mechanisms in the lithosphere and the origin of potassic alkaline magmas. Lithos. 28, 435-453.

Giacomuzzi, G., Civalleri, M., De Gori, P., Chiarabba, C., 2012. A 3D Vs model of the upper mantle beneath Italy: Insight on the geodynamics of central Mediterranean. Earth Planet. Sci. Lett. 335, 105-120.

González-Jiménez, J. M., Villaseca, C., Griffin, W. L., Belousova, E., Konc, Z., Ancochea, E., O'Reilly, S. Y., Pearson, N. J., Garrido, C. J., Gervilla, F., 2013. The architecture of the European-Mediterranean lithosphere: A synthesis of the Re-Os evidence. Geology. 41, 547-550.

Guo, Z., Wilson, M., Liu, J., Mao, Q., 2006. Post-collisional, potassic and ultrapotassic magmatism of the northern Tibetan Plateau: Constraints on characteristics of the mantle source, geodynamic setting and uplift mechanisms. J. Petrol. 47, 1177-1220.

Handy, M. R., M Schmid, S., Bousquet, R., Kissling, E., Bernoulli, D., 2010. Reconciling plate-tectonic reconstructions of Alpine Tethys with the geological–geophysical record of spreading and subduction in the Alps. Earth Sci. Rev. 102, 121-158.

Jackson, M. G. and Hart, S. R., 2006. Strontium isotopes in melt inclusions from Samoan basalts: implications for heterogeneity in the Samoan plume. Earth Planet. Sci. Lett. 245, 260-277.

Jochum, K. P., Weis, U., Stoll, B., Kuzmin, D., Yang, Q., Raczek, I., Jacob, D. E., Stracke, A., Birbaum, K., Frick, D. A., 2011. Determination of reference values for NIST SRM 610–617 glasses following ISO guidelines. Geostand. Geoanal. Res. 35, 397-429.

Jochum, K. P., Stoll, B., Herwig, K., Willbold, M., Hofmann, A. W., Amini, M., Aarburg, S., Abouchami, W., Hellebrand, E., Mocek, B., Raczek, I., Stracke, A., Alard, O., Bouman, C., Becker, S., Dücking, M., Brätz, H., Klemd, R., de Bruin, D., Canil, D., Cornell, D., de Hoog, C., Dalpé, C., Danyushevsky, L., Eisenhauer, A., Gao, Y., Snow, J. E., Groschopf, N., Günther, D., Latkoczy, C., Guillong, M., Hauri, E. H., Höfer, H. E., Lahaye, Y., Horz, K., Jacob, D. E., Kasemann, S. A., Kent, A. J. R., Ludwig, T., Zack, T., Mason, P. R. D., Meixner, A., Rosner, M., Misawa, K., Nash, B. P., Pfänder, J., Premo, W. R., Sun, W. D., Tiepolo, M., Vannucci, R., Vennemann, T., Wayne, D., Woodhead, J. D., 2006. MPI-DING reference glasses for in situ microanalysis: New reference values for element concentrations and isotope ratios. Geochem. Geophys. Geosyst. 7, Q02008.

Kay, R. W. and Kay, S. M., 1993. Delamination and delamination magmatism. Tectonophysics. 219, 177-189.

Kobayashi, K., Tanaka, R., Moriguti, T., Shimizu, K., Nakamura, E., 2004. Lithium, boron, and lead isotope systematics of glass inclusions in olivines from Hawaiian lavas: evidence for recycled components in the Hawaiian plume. Chem. Geol. 212, 143-161.

Koppel, V. and Schroll, E., 1985. Herkunft des Pb der triassischen Pb-Zn-Vererzungen in den Ost-und Südalpen; Resultate bleiisotopengeochemischer Untersuchungen. Arch. Lagerst. Forsch. Geol. Bundesanst. Wien. 6, 215-222.

Kramers, J. D. and Tolstikhin, I. N., 1997. Two terrestrial lead isotope paradoxes, forward transport modelling, core formation and the history of the continental crust. Chem. Geol. 139, 75-110.

Levin, V., Shapiro, N., Park, J., Ritzwoller, M., 2002. Seismic evidence for catastrophic slab loss beneath Kamchatka. Nature 418, 763-767.

Lustrino, M., 2005. How the delamination and detachment of lower crust can influence basaltic magmatism. Earth Sci. Rev. 72, 21-38.

Lustrino, M., Duggen, S., Rosenberg, C. L., 2011. The Central-Western Mediterranean: Anomalous igneous activity in an anomalous collisional tectonic setting. Earth Sci. Rev. 104, 1-40.

Lustrino, M., Melluso, L., Morra, V., 2007. The geochemical peculiarity of" Plio-Quaternary" volcanic rocks of Sardinia in the circum-Mediterranean area. Spec. Pap. Geol. Soc. Am.. 418, 277-301.

Lustrino, M., Melluso, L., Morra, V., 2000. The role of lower continental crust and lithospheric mantle in the genesis of Plio–Pleistocene volcanic rocks from Sardinia (Italy). Earth Planet. Sci. Lett. 180, 259-270.

Maclennan, J., 2008. Lead isotope variability in olivine-hosted melt inclusions from Iceland. Geochim. Cosmochim. Acta. 72, 4159-4176.

Malavieille, J., Chemenda, A., Larroque, C., 1998. Evolutionary model for Alpine Corsica: mechanism for ophiolite emplacement and exhumation of high-pressure rocks. Terra Nova. 10, 317-322.

Mason, P. R., Nikogosian, I. K., van Bergen, M. J., 2008. Major and trace element analysis of melt inclusions by laser ablation ICP-MS. Laser Ablation ICP–MS in the Earth Sciences: Current Practices and Outstanding Issues (P.Sylvester, Ed.). Mineral. Assoc. Can. Short Course Series. 40, 219-239.

Miller, C., Schuster, R., Klötzli, U., Frank, W., Purtscheller, F., 1999. Post-collisional potassic and ultrapotassic magmatism in SW Tibet: geochemical and Sr–Nd–Pb–O isotopic constraints for mantle source characteristics and petrogenesis. J. Petrol. 40, 1399-1424.

Moorbath, S., Taylor, P. N., Goodwin, R., 1981. Origin of granitic magma by crustal remobilisation: Rb-Sr and Pb/Pb geochronology and isotope geochemistry of the late Archaean Qôrqut Granite Complex of southern West Greenland. Geochim. Cosmochim. Acta. 45, 1051-1060.

Næraa, T., Kemp, A., Scherstén, A., Rehnström, E., Rosing, M., Whitehouse, M. J., 2014. A lower crustal mafic source for the ca. 2550Ma Qôrqut Granite Complex in southern West Greenland. Lithos. 192, 291-304.

Nikogosian, I. K., Elliott, T., Touret, J. L. R., 2002. Melt evolution beneath thick lithosphere: a magmatic inclusion study of La Palma, Canary Islands. Chem. Geol. 183, 169-193.

Nikogosian, I. K. and van Bergen, M. J., 2010. Heterogeneous mantle sources of potassium-rich magmas in central-southern Italy: Melt inclusion evidence from Roccamonfina and Ernici (Mid Latina Valley). J. Volcanol. Geotherm. Res. 197, 279-302.

Peccerillo, A., 2005. Plio-quaternary volcanism in Italy: Petrology, Geochemistry, Geodynamics. Springer-Verlag, Berlin, Germany.

Peccerillo, A., 1999. Multiple mantle metasomatism in central-southern Italy: geochemical effects, timing and geodynamic implications. Geology. 27, 315-318.

Peccerillo, A. and Martinotti, G., 2006. The Western Mediterranean lamproitic magmatism: origin and geodynamic significance. Terra Nova. 18, 109-117.

Portnyagin, M., Hoernle, K., Plechov, P., Mironov, N., Khubunaya, S., 2007. Constraints on mantle melting and composition and nature of slab components in volcanic arcs from volatiles (H< sub> 2 O, S, Cl, F) and trace elements in melt inclusions from the Kamchatka Arc. Earth Planet. Sci. Letters. 255, 53-69.

Prelević, D., Foley, S., Romer, R., Conticelli, S., 2008. Mediterranean Tertiary lamproites derived from multiple source components in postcollisional geodynamics. Geochim. Cosmochim. Acta. 72, 2125-2156.

Prelević, D., Jacob, D. E., Foley, S. F., 2013. Recycling plus: a new recipe for the formation of Alpine–Himalayan orogenic mantle lithosphere. Earth Planet. Sci. Lett. 362, 187-197.

Rose-Koga, E. F., Koga, K. T., Schiano, P., Le Voyer, M., Shimizu, N., Whitehouse, M. J., Clocchiatti, R., 2012. Mantle source heterogeneity for South Tyrrhenian magmas revealed by Pb isotopes and halogen contents of olivine-hosted melt inclusions. Chem. Geol. 334, 266-279.

Rosenbaum, G., Gasparon, M., Lucente, F. P., Peccerillo, A., Miller, M. S., 2008. Kinematics of slab tear faults during subduction segmentation and implications for Italian magmatism. Tectonics. 27, TC2008.

Rottura, A., Del Moro, A., Pinarelli, L., Petrini, R., Peccerillo, A., Caggianelli, A., Bargossi, G., Piccarreta, G., 1991. Relationships between intermediate and acidic rocks in orogenic granitoid suites: petrological, geochemical and isotopic (Sr, Nd, Pb) data from Capo Vaticano (southern Calabria, Italy). Chem. Geol. 92, 153-176.

Saal, A., Hart, S., Shimizu, N., Hauri, E., Layne, G., Eiler, J., 2005. Pb isotopic variability in melt inclusions from the EMI–EMII–HIMU mantle end-members and the role of the oceanic lithosphere. Earth Planet. Sci. Lett. 240, 605-620.

Scrocca, D., 2006. Thrust front segmentation induced by differential slab retreat in the Apennines (Italy). Terra Nova. 18, 154-161.

Serri, G., Innocenti, F., Manetti, P., 1993. Geochemical and petrological evidence of the subduction of delaminated Adriatic continental lithosphere in the genesis of the Neogene-Quaternary magmatism of central Italy. Tectonophysics. 223, 117-147.

Sobolev, A., Dmitriev, L., Barsukov, V., Nevsorov, V., Slutskii, A., 1980. The formation conditions of the high-magnesium olivines from the monomineralic fraction of Luna 24 regolith. Lunar Planet. Sci. Conf. Proc. 11, 105-116.

Sobolev, A. V., Hofmann, A. W., Nikogosian, I. K., 2000. Recycled oceanic crust observed in 'ghost plagioclase' within the source of Mauna Loa lavas. Nature. 404, 986-990.

Sorbadere, F., Schiano, P., Métrich, N., 2012. Constraints on the origin of nepheline-normative primitive magmas in island arcs inferred from olivine-hosted melt inclusion compositions. J. Petrol. egs063.

Spakman, W., Wortel, M.J.R., 2004. A tomographic view on western Mediterranean geodynamics, in: Cavazza W., et al. (Eds), The TRANSMED atlas. The Mediterranean region from crust to mantle. Springer, pp. 31-52.

Stos-Gale, Z., Gale, N. H., Houghton, J., Speakman, R., 1995. Lead isotope data from the Isotrace Laboratory, Oxford: Archaeometry Data Base 1, ores from the Western Mediterranean. Archaeometry. 37, 407-415.

Tommasini, S., Avanzinelli, R., Conticelli, S., 2011. The Th/La and Sm/La conundrum of the Tethyan realm lamproites. Earth Planet. Sci. Lett. 301, 469-478.

Whitehouse, M. J., Kamber, B. S., Fedo, C. M., Lepland, A., 2005. Integrated Pb-and S-isotope investigation of sulphide minerals from the early Archaean of southwest Greenland. Chem. Geol. 222, 112-131.

Wortel, M.J.R. and Spakman, W., 2000. Subduction and slab detachment in the Mediterranean-Carpathian region. Science. 290, 1910-1917.

Zhao, Z., Mo, X., Dilek, Y., Niu, Y., DePaolo, D. J., Robinson, P., Zhu, D., Sun, C., Dong, G., Zhou, S., 2009. Geochemical and Sr–Nd–Pb–O isotopic compositions of the post-collisional ultrapotassic magmatism in SW Tibet: petrogenesis and implications for India intra-continental subduction beneath southern Tibet. Lithos. 113, 190-212.

Figure Captions

Figure 1. **a**: Location of Latera volcano and other volcanic centers of central-southern Italy. Map redrawn after Peccerillo (2005). RMP: Roman Magmatic Province, TMP: Tuscan Magmatic Province, ERMP: Ernici-Roccamonfina Magmatic Province, CMP: Campanian Magmatic province. Orange curve marks Alpine subduction and blue curve marks Apennine subduction, including Calabrian subduction in the southern part. **b**: Schematic representation of tomographic model for mantle structure with subducted slabs beneath Italy and Tyrrhenian Sea, after Spakman and Wortel (2004), and approximate position of the mantle column below Latera volcano.

Figure 2. Variation diagrams for lavas and melt inclusions (MIs) of Selva del Lamone and Mt. Starnina of **a**: K_2O vs. CaO, **b**: MgO vs. CaO, **c**: MgO vs. Pb, d: Th/Ba vs. Pb/Nd normalized to depleted MORB mantle (DMM). Symbols refer to different groups of MIs in the Selva del Lamone (SdL) and Monte Starnina lavas. Fields for shoshonite (SHO) and lamproite (LAM) volcanic rocks from Latera and Tuscany, respectively, and for silica-undersaturated leucite-bearing high-potassic series rocks (HKS) from Vulsini are based on data from Conticelli et al. (1991) and Lustrino et al. (2011). Note that the measured compositions of Group-2 MIs were not corrected for possible post-entrapment re-equilibration so that original MgO concentrations might have been lower than shown in the plots. Arrows in **b** and **c** indicate direction of melt evolution predicted by crystal fractionation of olivine and/or clinopyroxene. Hence, crystal fractionation cannot have produced the difference between the MI groups from SdL, whereas the bulk lava composition can be explained as a slightly evolved mixture of the two. The trace element ratios in d represent pairs with comparable incompatibility and are

shown to illustrate that Group-2 melts were derived from a compositionally distinct mantle source.

Figure 3. Pb isotope data for melt inclusions from the SdL and Monte Starnina lavas. **a:** $^{207}Pb/^{204}Pb$ vs. $^{206}Pb/^{204}Pb$ comparing compositions of MIs with data for Late Archean granitoids from West Greenland (orange stars) that were derived from a crustal source with (at least partly) an Eoarchean age (Moorbath et al., 1981; Næraa et al., 2014); note that the unradiogenic endmember of the Group-1 MIs overlaps with the radiogenic end of the granitoid array. **b:** $^{207}Pb/^{204}Pb$ vs. $^{206}Pb/^{204}Pb$ for MIs from the SdL and Monte Starnina lavas. **c:** Close up of b. together with fields for bulk lavas from the northern Roman Magmatic Province HKS, Latera SHO, and the Tuscan Magmatic Province (Lustrino et al., 2011) and for basement rocks in the region. The Calabrian basement is represented by granitoids (Rottura et al., 1991), the Sardinian basement by K-Feldspars from pre-Variscan sandstones and granites (Caron et al., 1997) and sulfides (Stos-Gale et al., 1995), and the Alpine sandstone by K-feldspars and galenites from the Permian Grödener sandstones, East Alps (Koppel and Schroll, 1985). The isotopic closeness of the Group-2 MIs to Sardinian and Calabrian basement rocks and the Permian sandstone suggests that these lithologies or their erosion products contaminated the mantle source below Latera via the Alpine subduction system. Conversely, the signatures of the Group-1 and Mt. Starnina MIs point to a superimposed imprint from the Apennine subduction. **d:** $^{208}Pb/^{204}Pb$ vs. $^{206}Pb/^{204}Pb$ for MIs from the SdL and Monte Starnina lavas. **e:** $^{208}Pb/^{206}Pb$ vs. $^{207}Pb/^{206}Pb$ for MIs from the SdL and Monte Starnina lavas; Magmatic provinces: TMP=Tuscan, RMP=Roman, ERMP=Ernici-Roccamonfina, CMP=Campanian (Lustrino et al., 2011). Symbols as in Fig.2. Error bars, where larger than the symbol size, represent 2-sigma

uncertainties based on the standard error of the mean. The diagonal error bars in the isotope plots are due to the highly correlated errors of ^{204}Pb-based ratios. Dashed line in each panel is the Northern Hemisphere Reference Line. UCC=upper continental crust, LCC=lower continental crust.

Figure 1

Click here to download high resolution image

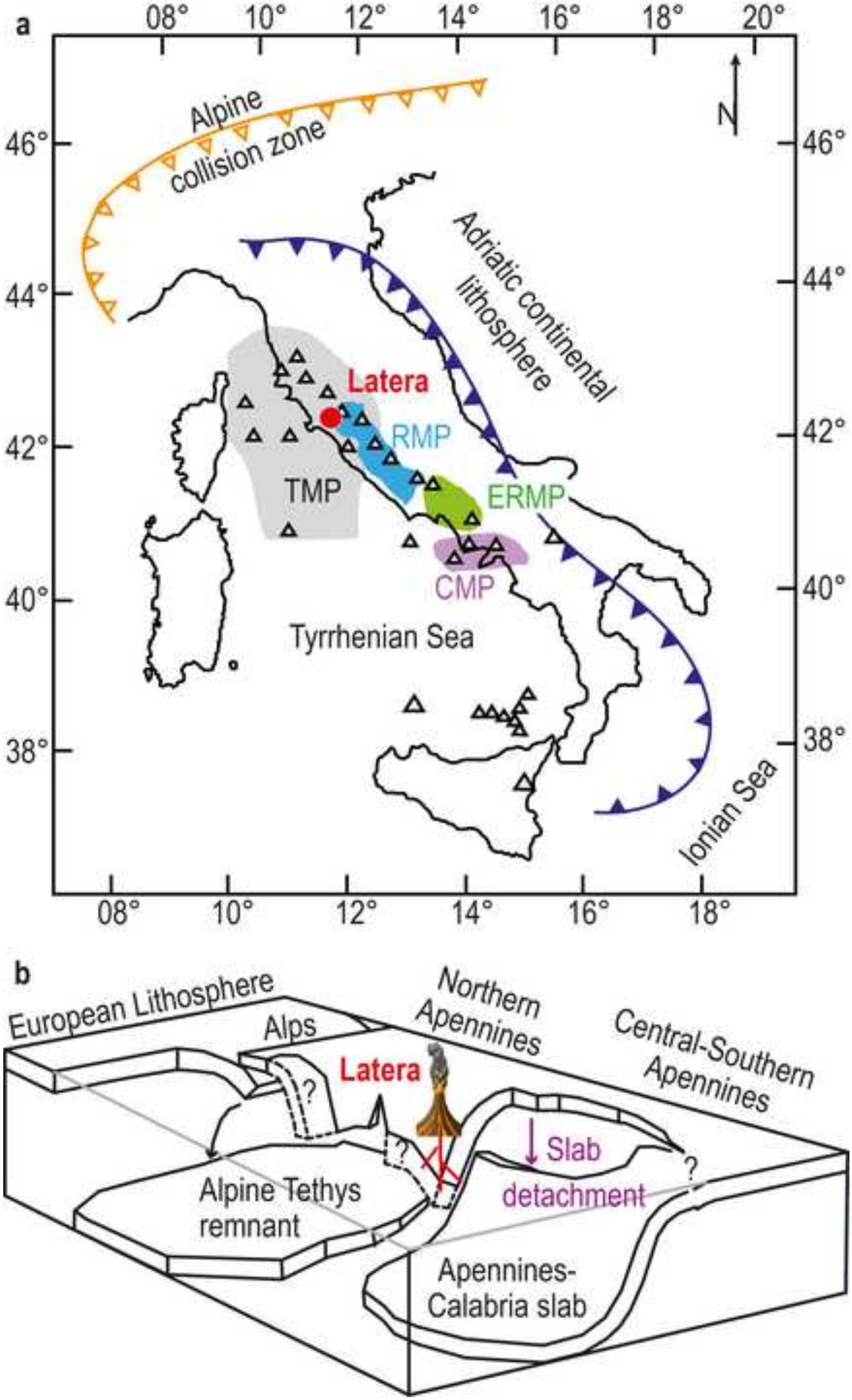

Figure 2

Click here to download high resolution image

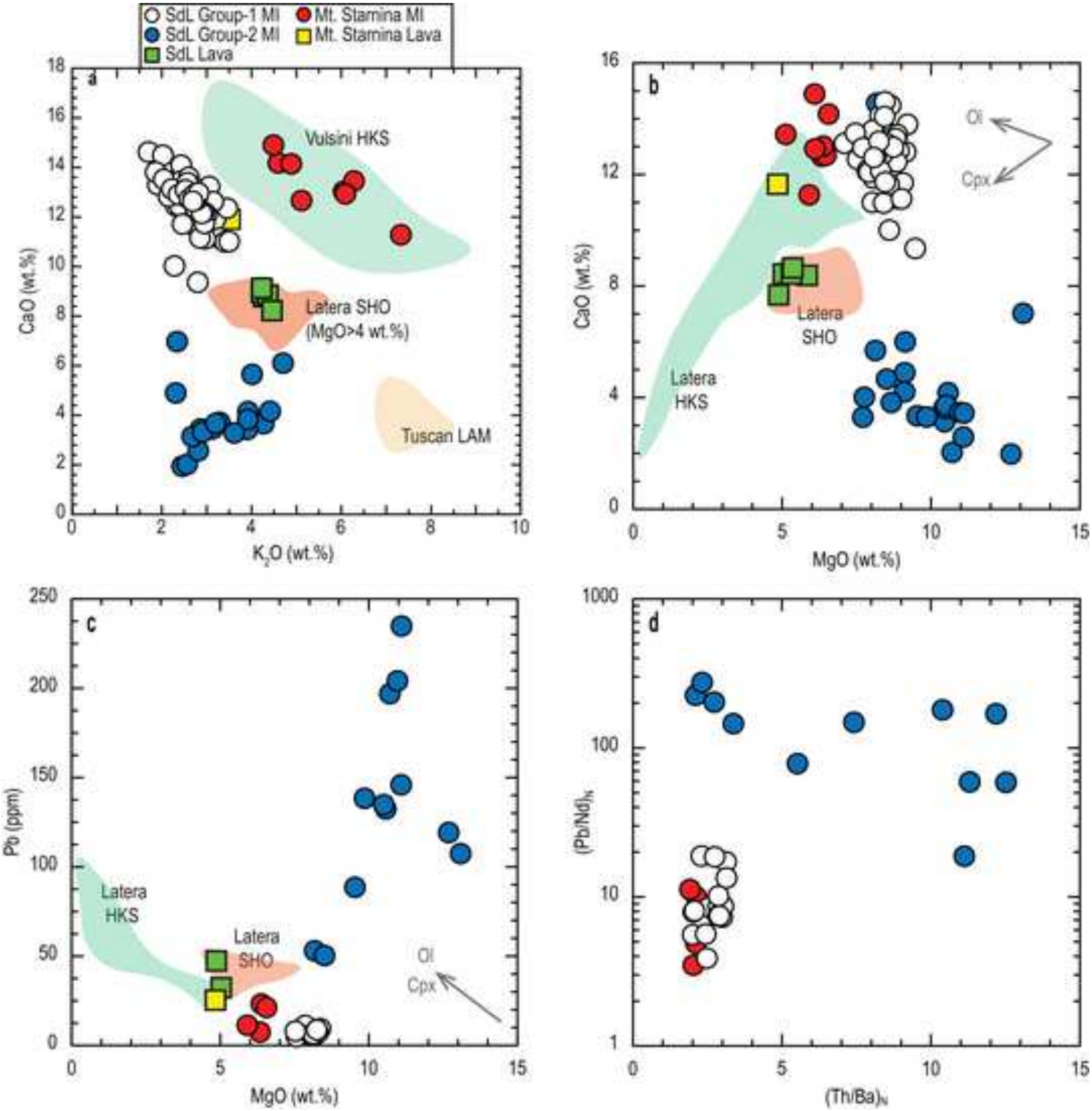

Figure 3

Click here to download high resolution image